1.1 STABILITY OF STRENGTHENING PRECIPITATES IN MODEL FERRITIC STEELS —

L. Tan (Oak Ridge National Laboratory)

OBJECTIVE

Evaluate the stability of a variety of candidate strengthening precipitates in RAFM steels under thermal, stress, and radiation conditions, based on experimental observation coupled with computational thermodynamics and kinetics simulations.

SUMMARY

The effect of thermal aging, creep, and irradiation on the stability of strengthening precipitates including VN, TaN, and TaC are being systematically evaluated. Three model alloys, Fe-1WVN, Fe-1WTaN, and Fe-1WTaC, have been designed and fabricated. Nano-precipitates of VN, TaN, and TaC with sizes ~9 – ~19 nm and densities in the orders of 10^{20} – 10^{22} m^{-3} were developed in these alloys. These nano-precipitates will serve as good initial point for investigating their stabilities under different tests. Free dislocation densities were characterized in the order of 10^{13} – 10^{14} m^{-2}. Tensile tests of the control samples have been completed, which results will be used as benchmarks for the aging and irradiation experiments. Thermal aging of the alloys at 600°C and 700°C for 100 h has been completed. Creep testing of a Fe-1WTaC sample at 600°C and 170 MPa (~70% yield strength) has been completed. The microstructures of the tested samples are being characterized. Longer time thermal aging and creep tests of the other samples are in progress. Self-ion (Fe^{2+}) irradiation of the samples has been planned at 500°C and 700°C for 20 dpa and 200 dpa. Tensile samples of the alloys have been prepared for neutron irradiation at 300°C, 500°C, and 650°C for up to ~20 dpa.

PROGRESS AND STATUS

Introduction

High-temperature aging-induced softening is one of the issues of ferritic-martensitic (FM) steels. It has been observed that reduced activation ferritic-martensitic (RAFM) steel F82H suffered aging-induced softening at temperatures above ~550°C, which was more than 30% after aging at 650°C for more than ~10,000 h [1]. The softening is primarily a result of the weakened pinning effect of coarsened or disappeared precipitates leading to recovery of dislocation substructures. Similar to conventional FM steels, there are three major types of precipitates in F82H. $M_{23}C_6$ and Laves phase are two types of predominant precipitates. Extensive studies have been pursued on the stability of these two types of precipitates. Significant coarsening occurs in both $M_{23}C_6$ and Laves phase, reaching a size greater than ~300 nm, despite the usually delayed appearance of Laves phase. The third type precipitates, MX with M = metals and X = C/N, are excellent strengthening phase due to their ultrafine size in tens of nanometers or smaller. Limited literature data suggested superior stability of TaC followed by TaN and VN under thermal and/or stress conditions [2,3]. Preliminary heavy ion irradiation experiments, however, suggested instability of TaC under Fe^{3+} ion irradiation at 500°C for 20 dpa (displacement per atom) [4]. This study is to screening the stability of candidate strengthening precipitates in RAFM steels under thermal, stress, and radiation conditions. The outcome of this study will help understanding the degradation mechanisms of RAFM steels induced by precipitates evolution, and more importantly provide invaluable insights for developing advanced RAFM steels.

Experimental Procedure

Model Alloy Design and Fabrication

Three model alloys, i.e., Fe-1WVN, Fe-1WTaN, and Fe-1WTaC, have been designed using computational thermodynamics to favor the formation of VN, TaN, and TaC in respective alloys. The calculated phase fraction as a function of temperature for the model alloys is shown in Fig. 1. Two types of precipitates, i.e., Laves phase Fe_2W and MX (VN, TaN, and TaC), exist in the model alloys. Chromium is not added in the model alloys to prevent the difficulty during microstructural characterization during transmission electron microscopy (TEM) because of the similar size between $M_{23}C_6$ and Fe_2W. It is assumed that the nonexistence of chromium will not influence the stability of MX because chromium is the primary element forming $M_{23}C_6$ and may promote the coarsening of $M_{23}C_6$ and Fe_2W.

One ingot (~4.5 kg) was casted using vacuum induction melting (VIM) for each model alloy. A ~19 mm thick plate was obtained from each ingot by hot forging, hot rolling, normalization, and tempering. The same normalization and tempering temperatures, 1200°C and 750°C, respectively, were applied to the plates.

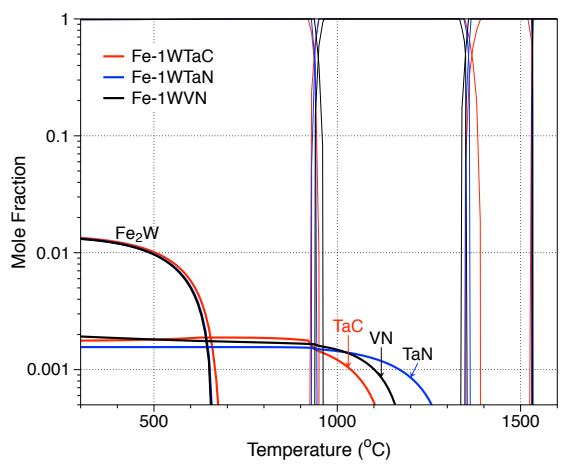

Fig. 1. Calculated phase fraction as a function of temperature for the three model alloys.

Stability Screening

Three types of testing conditions, i.e., thermal aging, creep, and irradiation, are planned for screening the stability of the strengthening precipitates. Thermal aging experiments have been started at 600°C and 700°C with times from 100 h to 5000 h. Possible effect of Laves phase on MX stability will be assessed at the 600°C aging condition. Creep tests will be conducted at two levels of loading stress, e.g., ~70% and ~40% yield strength. Both neutron irradiation and heavy ion irradiation experiments are planned for the model alloys.

Microstructure Characterization

The microstructures of the samples prior to and after the screening experiments are primarily characterized using TEM. Other supplementary techniques such as energy dispersive X-ray

spectroscopy (EDS), scanning electron microscopy (SEM) and optical microscopy are also employed.

Results

Alloys in the Control Condition

Optical micrographs in Fig. 2 indicate that the Fe-1WTaN alloy has slightly smaller grain size than the other two alloys. Many nano-precipitates were observed in the alloy as shown in the bright-field TEM images of Fig. 2. Very few free dislocations were observed within the grains of these alloys. The statistical results of the size and volume number densities of these nano-precipitates and the density of free dislocations are listed in Table 1. The size of VN precipitates was about twice of the TaN and TaC precipitates. The density of TaN was in the order of 10^{22} m^{-3}, one order of magnitude greater than that of TaC and two orders of magnitude greater than that of VN. The large deviation of the VN density was a result of the non-uniform distribution of the particles with Fig. 3 as an example. Similar free dislocation density in the order of 10^{14} m^{-2} was observed in the Fe-1WTaN and Fe-1WTaC alloys, which is comparable to tempered P91 of ~5×10^{14} m^{-2}. The dislocation density in the Fe-1WVN alloy was about one order of magnitude lower than the other two alloys.

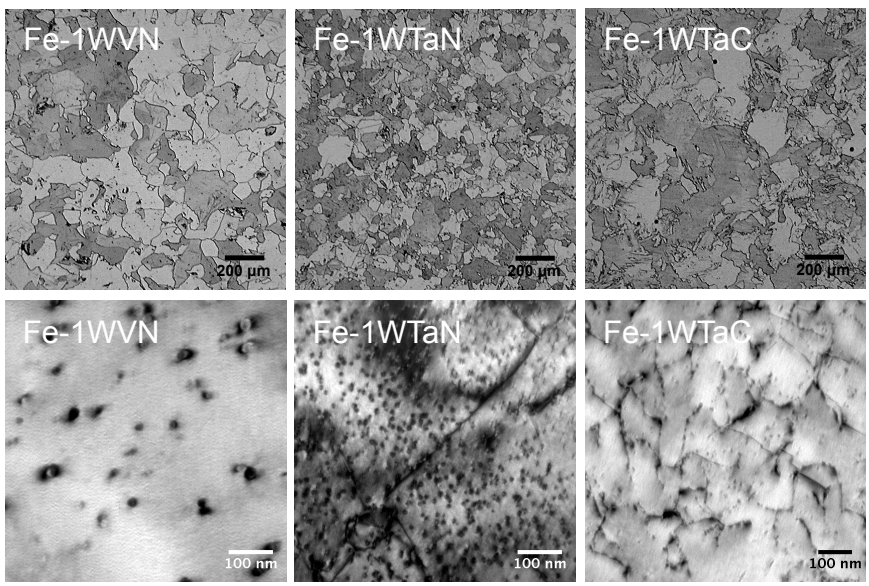

Fig. 2. Optical micrographs (first row) and bright-field TEM images (second row) of the model alloys.

Table 1. Statistical results of the precipitates and free dislocations in the model alloys.

Microstructural Feature		Fe-1WVN	Fe-1WTaN	Fe-1WTaC
Particle	Type	VN	TaN	TaC
	Size (nm)	18.6±3.1	9.1±2.3	9.7±1.9
	Density ($\times10^{21}$ m^{-3})	0.396±0.290	19.3±4.56	3.41±0.76
Dislocation	Density ($\times10^{14}$ m^{-2})	0.22±0.04	1.30±0.26	1.80±0.31

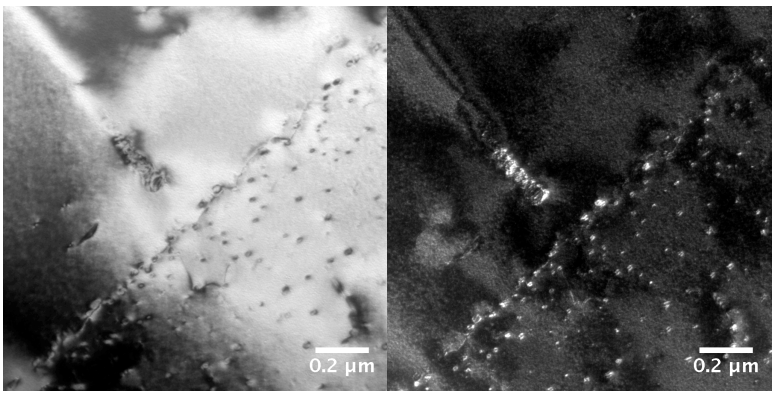

Fig. 3. Bright-field and dark-field TEM images showing non-uniform distribution of VN in alloy Fe-1WVN.

The yield strength data of the three model alloys at temperatures up to 700°C are plotted in Fig. 4. The data of RAFM steel F82H from Ref. [5] are included for comparison. The model alloys exhibited lower yield strength than F82H because of their fewer strengthening elements such as sub-boundary strengthening and solution strengthening from W, Cr, etc. However, Fe-1WTaC and Fe-1WTaN showed yield strength comparable to F82H at temperatures above 600°C. Alloy Fe-1WVN had the lowest strength due to the smaller densities of both strengthening particles VN and dislocations. The particle strengthening and dislocation strengthening were estimated using the equations of σ_P (GPa) = $1.1Gb(r \times n)^{1/2}$ and σ_D (GPa) = $0.5Gb\rho^{1/2}$, respectively, where G is shear modulus (80.2 GPa for iron), b the magnitude of Burger's vector (2.49×10^{-10} m for iron), r the radium of particles, n the density of particles, and ρ the density of free dislocations. The calculated results are summarized in Table 2. The particle and dislocation strengthening contributed ~38%, ~66%, and ~56% to the yield strength of Fe-1WVN, Fe-1WTaN, and Fe-1WTaC, respectively.

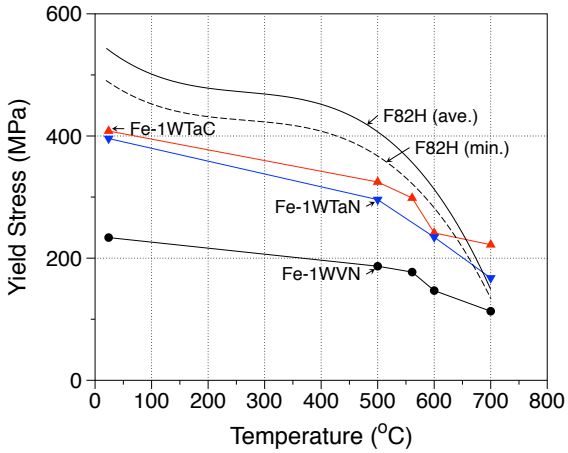

Fig. 4. Yield strength of the model alloys at temperatures up to 700°C.

Table 2. Calculated strength contributions from particles and free dislocations.

Stress (MPa)	Fe-1WVN	Fe-1WTaN	Fe-1WTaC
σ_P (particle)	42	157	89
σ_D (dislocation)	47	114	134

Thermal Aging

Thermal aging experiments on the model alloys at 600°C and 700°C have completed 100 h. The aging effect on yield strength of the alloys is shown in Fig. 5. Some variation in yield strength occurred in the alloys. Microstructural evolution induced by the aging is being characterized. The aging for 1,000 h and 5,000 h is in progress.

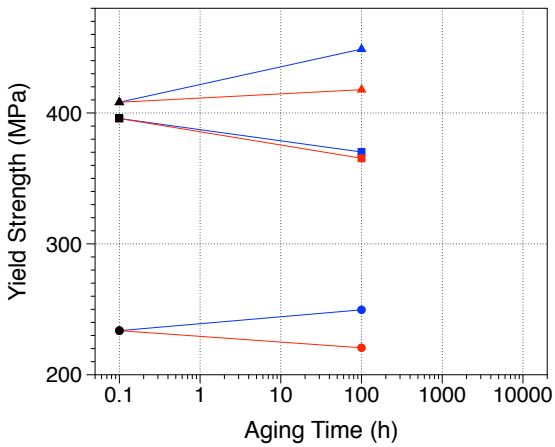

Fig. 5. Effect of thermal aging at 600°C (blue) and 700°C (red) on yield strength of Fe-1WVN (circles), Fe-1WTaN (squares), and Fe-1WTaC (triangles).

Creep Testing

A creep test of a Fe-1WTaC sample was conducted at 600°C and 170 MPa (~70% yield strength). Its creep life (371 h) is comparable to F82H [6] as shown in Fig. 6. The microstructural of the crept sample is being characterized. Creep tests of the other alloys are in progress.

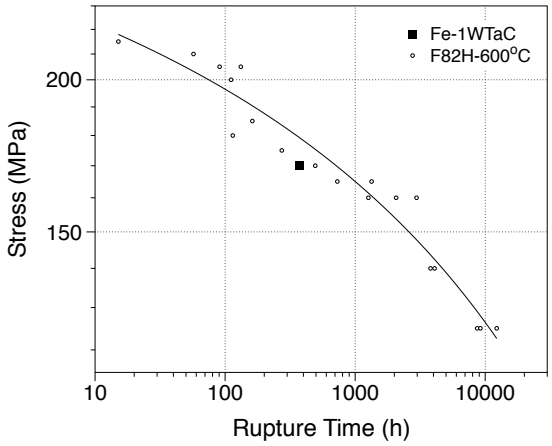

Fig. 6. Creep rupture time of Fe-1WTaC at 170 MPa load.

Heavy Ion and Neutron Irradiation

Self-ion (Fe^{2+}) irradiation of the samples is planned at 500°C and 700°C for 20 dpa and 200 dpa, using the ion beam facility at University of Michigan through ATR National Science User Facility (ATR-NSUF).

Type SS-J2 tensile samples of the alloys had been prepared and incorporated into the US-Japan irradiation campaign, which will be irradiated in the High Flux Isotope Reactor (HFIR) at 300°C, 500°C, and 650°C for up to ~20 dpa. The irradiation conditions and number of samples are listed in Table 3.

Table 3. Number of type SS-J2 samples planned for neutron irradiation in HFIR.

Capsule ID	Temperature (°C)	Fluence ($\times 10^{25}$ n/m^2)	Fe-1WVN	Fe-1WTaN	Fe-1WTaC
TB-300-2	300	0.1	1	1	1
TB-300-3		0.5	1	1	1
TB-300-4		7	1	1	1
TB-500-1	500	0.1	1	1	1
TB-500-2		0.5	1	1	1
TB-500-3		7	1	1	1
TB-650-1	650	0.1	1	1	1
TB-650-2		0.5	1	1	1
TB-650-3		7	1	1	1
TB-650-4		20	1	1	1

REFERENCES

[1] H. Tanigawa, K. Shiba, A. Möslang, R. E. Stoller, R. Lindau, M. A. Sokolov, G. R. Odette, R. J. Kurtz, and S. Jitsukawa, *J. Nucl. Mater.* **417** (2011) 9-15.
[2] M. Tamura, H. Sakasegawa, A. Kohyama, H. Esaka, and K. Shinozuka, *J. Nucl. Mater.* **329** (2004) 328.
[3] A. Kabadwal, M. Tamura, K. Shinozuka, and H. Esaka, *Metall. Mater. Trans. A* **41** (2010) 364.
[4] H. Sakasegawa, et. al., "Microstructural changes of finely dispersed MX precipitates in ion-irradiated ferritic heat –resistant steels," presented in the Conference of Japan Institute of Metals, Sept. 22-24, 2001.
[5] A.-A. F. Tavassoli, J.-W. Rensman, M. Schirra, and K. Shiba, *Fusion Eng. Des.* **61** (2002) 617.
[6] N. Yamanouchi, M. Tamura, H. Hayakawa, A. Hishinuma, and T. Kondo, *J. Nucl. Mater.* **191** (1992) 822.